67º congresso 2012 abm
67th abm international congress
ISSN 1516-392X

KINECTS AND STRUCTURAL EVOLUTION OF 304L STAINLESS STEEL WITH TRIP EFFECT WHEN SUBMITTED TO UNIAXIAL TENSILE TEST UNDER DISTINCT STRAIN RATES [1]

Andersan dos Santos Paula[2]
Marcelo Costa Cardoso[3]
Thiago Farias Vieira[4]
Jéssica Gonçalves Andrade[5]
Guilherme Almeida Monteiro[6]
Luciano Pessanha Moreira[7]
Maria Carolina dos Santos Freitas[8]

Abstract
The martensitic transformation in austenitic stainless steels can be induced by plastic deformation at room and lower temperatures. In this study, a systematic series of experiments was conducted to assess the influence of strain level and strain-rate in uniaxial stress at room temperature correlating the mechanical properties with the microstructural changes associated to the phase transformation and/or strain hardening. The experimental results allowed to estimate the effect of deformation on martensitic transformation and microstructural evolution in metastable 304L austenitic stainless steel under uniaxial tensile loading at room temperature.
Key words: Kinetic; Structural evolution; TRIP effect; Tensile test.

CINÉTICA E EVOLUÇÃO ESTRUTURAL DE AÇO INOXIDÁVEL 304L COM EFEITO TRIP QUANDO SUBMETIDO A ENSAIO DE TRAÇÃO UNIAXIAL SOB DISTINTAS TAXAS DE DEFORMAÇÃO

Resumo
A transformação martensítica em aços inoxidáveis austeníticos pode ser induzida por deformação plástica a temperatura ambiente e inferiores a esta. Neste estudo foram conduzidos uma série de experimentos de modo verificar a influência do nível e da taxa de deformação durante ensaio de tração uniaxial a temperatura ambiente correlacionando as propriedades mecânicas com as mudanças microestruturais associadas a transformação de fase e/ou encruamento. Os resultados do presente estudo permitiram estimar o efeito da deformação na transformação martensítica e evolução microestrutural em um aço inoxidável austenítico metaestável 304L submetido a ensaio de tração uniaxial a temperatura ambiente.
Palavras-chave: Cinética; Evolução estrutural; Efeito TRIP; Ensaio de tração.

[1] *Technical contribution to 67th ABM International Congress, July, 31th to August 3rd, 2012, Rio de Janeiro, RJ, Brazil.*
[2] *D.Sc., Professor at VMT and PPGEM / UFF, Volta Redonda, RJ, Brazil.*
[3] *B.Sc. Engineer, M.Sc. Student at PPGEM / UFF, Volta Redonda, RJ, Brazil.*
[4] *B.Sc. Student – Metallurgical Engineering at VMT / UFF, Volta Redonda, RJ, Brazil.*
[5] *B.Sc. Student – Metallurgical Engineering at VMT / UFF, Volta Redonda, RJ, Brazil.*
[6] *B.Sc. Student – Mechanical Engineering at VEM / UFF, Volta Redonda, RJ, Brazil.*
[7] *D.Sc., Professor at VEM and PPGEM / UFF, Volta Redonda, RJ, Brazil.*
[8] *M.Sc, PhD Student at PPGEM / UFF, Professor at UniFOA, Volta Redonda, RJ, Brazil.*

ISSN 1516-392X

1 INTRODUCTION

Phase transformations are crystallographic process accompanied of diffusion and/or diffusionless. Martensite is a nonequilibrium single-phase structure that results from a diffusionless transformation of a high temperature parent phase (austenite, in case of ferrous alloys).
According to Cohen and Wayman,[1] "martensitic reactions are a subclass of displacive, diffusionless phase transformations in which the kinetics and morphology are dominated by relatively large shearlike displacements in the transforming micro-regions". The resulting local shape changes involve both lattice (homogeneous) and lattice-invariant (inhomogeneous) deformations, the former being accomplished by coherency (or transformation) dislocations and the latter by anticoherency (or misfit) dislocations. Both types of dislocations move glissilely and comprise the interfacial structure.
Some alloying elements (C, Ni and Mn have strong effects) stabilize the austenite in ferrous alloys, expanding it domain, reducing the minimum temperature at which the austenite is stable, which are expected to lower the start (M_s) and finish (M_f) temperatures for the martensitic transformation in order to attain the necessary degree of undercooling. The carbide formers, Mo and Cr, also lower the M_s temperature even though they are ferrite stabilizers and would be expected to enhance the driving force for the transformation. Presumably, these alloying elements cause changes that make the transformation more difficult. It is not clear what these changes are. It is possible that the initiation sites are affected by inhomogeneous austenite matrix produced by precipitation. Solid solution strengthening of the austenite and changes to its shear modulus which might resist the necessary shape change may contribute. Nevertheless, all five elements lower the martensitic start temperature.[2] The alloying elements relative effects on M_s temperature can be estimated by empiric relations:[3]

$$M_s\ (^oC) = 1350 - 1665(\%C+\%N) - 28(\%Si) - 33(\%Mn) - 42(\%Cr) - 61(\%Ni) \quad (1)$$

Martensitic transformation can be induced by application of stress as well as by changes in temperature. Both temperature and stress are macroscopic variables that affect the transformation because they influence the thermodynamics and kinetics of the transformation. Moreover, the thermodynamic and kinetic effects and, thus, the overall response of the material, are strongly dependent on micro scale mechanisms governed by couplings between stress and different strain mechanisms (plastic flow of product and parent phases, transformation strain field) which are at the origin of orientation and accommodation effects.[4-8]
Transformation induced plasticity (TRIP), in its "classical" definition, can be explained as the "… significantly increased plasticity during a phase change. For an externally applied load for which the corresponding equivalent stress is small compared to the normal yield stress of the material, plastic deformation occurs …". This definition can be found in the review work by Fischer et al.[9,10]
The transformation induced plasticity deals with at least two inter related inelastic strain mechanisms: plastic flow by dislocation motion and the inelastic transformation strain related with the martensitic phase change. In addition to the usual thermoelastic properties which may be assumed homogeneous for usual TRIP materials like steels, the plastic behavior of an austenitic-martensitic two-phase material appears strongly heterogeneous.[4] Strain rate applied and the heat

ISSN 1516-392X

produced during cold working affect the TRIP effect, as increasing them, the martensite nucleation decreases and dislocation density increases.
The highest temperature to which the M_s temperature can be raised by applied stresses is defined as the M_d temperature.[11,12] This temperature was first identified by McReynolds.[13] When this temperature lies above room temperature and the M_s is below room temperature, it is possible to retain the austenite at room temperature and then, some martensite can be formed by working the metastable austenite at room temperature. This can be important in highly alloyed steels such as stainless steels.
In austenitic stainless steels, cold work generally produces a phase transformation from face-centred-cubic (fcc), γ-austenite, to body-centred-cubic (bcc), α'-martensite,[5] where martensite is stronger than austenite resulting higher strength material after the martensitic transformation. The extent of α'-martensitic transformation depends on several factors that will be considered in turn. The most important factors are the chemical composition and the temperature at which plastic deformation takes place. The direct effect of the composition on the formation of strain-induced martensite on alloy 304 was first investigated by Angel,[6,7,14] who correlated elemental compositions with the temperature at which half of the austenite is transformed by the application of 0.3 true strain in tension, denoted by M_{d30}, i.e.

$$M_{d30}\ (^{o}C) = 413 - 462(\%C + \%N) - 9.2(\%Si) - 8.1(\%Mn) - 13.7(\%Cr) - 9.5(\%Ni) - 18.5(\%Mo) \quad (2)$$

The aim of the present work was to study the kinetic and structural evolution of the 304L austenitic stainless steel with TRIP effect when submitted to mechanical loading at room temperature. The samples of this material were submitted to uniaxial tensile tests at room temperature under two strain rates ($5{,}55 \times 10^{-4}$ and $5{,}55 \times 10^{-3}\ s^{-1}$), in parallel to *in-situ* measure of martensite formation by a ferritoscope during tests stops between yield and maximum load. The structural characterizations were performed in as-received condition and after tensile tests with distinct interrupted conditions. X-Ray Diffraction (XRD), Scanning Electronic Microscopy (SEM), and Vickers Microhardness test were used to evaluated the present phases and phase transformation, microstructural and mechanical evolution due to TRIP effect.

2 MATERIAL AND METHODS

2.1 Material

The material in this study is an austenitic stainless steel sheet, classified as 304 L, supplied by Arcelor Mittal Inox of Brasil S.A. According to the supplier data, the material was hot rolled up to 2.85 mm thickness, cold rolled up to 1.0 mm thickness and 500 mm width and submitted to box annealing at 1,060ºC (soaking temperature). The chemical composition is shown in the Table 1, associated with M_s[3] and M_{d30}[6] equals to 4,11 and 61,72ºC, respectively, calculated by Equations 1 and 2.

Table 1. Chemical composition of the austenitic stainless steel sheet in study

Element (% in weight)								
C	Mn	Si	P	S	Cr	Ni	Mo	Al
0.018	1.2693	0.4786	0.0303	0.0015	18.3639	8.0221	0.0261	0.0032
Cu	Co	V	Nb	Pb	B	Ti	Sn	W
0.0428	0.1015	0.0418	0.0071	0.001	0.006	0.0018	0.0044	0.0146

ISSN 1516-392X

2.2 Methods

The material in study was characterized in as-received (AR) condition, during and after tensile tests proposed in the present work. The characterizations employed in AR and tensile test samples were microstructural analysis by Scanning Electronic Microscopy (SEM) and X-Ray Diffraction (XRD), mechanical properties evaluation by microhardness Vickers and uniaxial tensile tests, and phase transformation by XRD and in-situ magnetic measurements during uniaxial tensile tests using a ferritoscope.
In order to study the effect of the strain rate on martensitic transformation kinetics and structural evolution, tensile specimens were cut from rolling direction (RD), and pulled in 12 distinct conditions described in Table 2. The tensile tests were performed in a universal machine (EMIC DL-1000) with loading cell of 10,000 Kg, installed in UNIFOA / Brazil. The ferristoscope in-situ measurements on middle of gauge length (Figure 1) were only applied during tensile test with stop condition below maximum load (ML) (Table 2 – IN-L1 to IN-L11 samples).

Table 2. Tensile Test conditions performed in present work at room temperature

Samples	Stop Condition / Load (N)	Strain-rate (s^{-1})
IN-L	Up to break (Rupture)	5.55×10^{-4}
IN-L1	Up to break (Rupture)	5.55×10^{-3}
IN-L2	YL + (ML – YL) * 0.9 = 9000 (90%)	5.55×10^{-4}
IN-L3	YL + (ML – YL) * 0.5 = 7300 (50%)	
IN-L4	YL + (ML – YL) * 0.1 = 5600 (10%)	
IN-L5	YL + (ML – YL) * 0.75 = 8150 (75%)	
IN-L6	YL + (ML – YL) * 0.25 = 6450 (25%)	
IN-L7	YL + (ML – YL) * 0.9 = 8500 (90%)	5.55×10^{-3}
IN-L8	YL + (ML – YL) * 0.5 = 7250 (50%)	
IN-L9	YL + (ML – YL) * 0.1 = 5980 (10%)	
IN-L10	YL + (ML – YL) * 0.75 = 7880 (75%)	
IN-L11	YL + (ML – YL) * 0.1 = 6630 (25%)	

YL = Yielding load; ML = Maximum load.

The samples, after tensile tests, for the metallographic analysis, microhardness tests and X-Ray Diffraction analysis were extracted from tensile specimen gauge length assisted by diamond disc cut installed on ISOMET Buehler cutting machine, as showing in Figure 1.

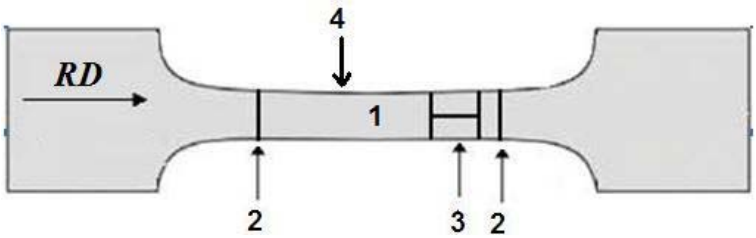

Figure 1. Schematic drawing tensile specimen measurements and cut marks. 1 - Ferritoscope measurement point on middle of gauge length; 2 - cut marks with ISOMET cutting machine; 3 - Metallographic and microhardness sample on RD; 4 - XRD sample.

The samples for metallographic analysis and microhardness tests were pressed in cold cure metallographic resin, and wet sanding followed by mechanical polishing with diamond past (6μm, 3μm and 1 μm) and alumina (0.05 μm). The microstructures were revealed by immersion on chemical solution with nitric acid, chloridric acid and water distilled in 1:1:1 volume proportion.

ISSN 1516-392X

The samples were observed on Scanning Electronic Microscopy (SEM) – Zeiss EVO MA10, with LaB6 filament, installed in EEIMVR/UFF (Electronic Microscopy Multiuser Laboratory - LMME). Vickers Microhardness tests were proceeding in the samples in study using a microhardness tester Buhler LTD model Micromet 3, installed in EEIMVR/UFF. The test load and creep time were 300 gf and 20 s, respectively; for each sample, 10 measurements were performed in ¼ thickness sample line.
The present phases (austenite and martensite) in steel samples in study at as-received and tensile specimens were determined by XRD beyond ferritoscope measurements, in order to observe the phase transformation kinetic associated with modifications on profile of the austenitic peaks consumed and martensitic peaks formed. The diffractometer used is XRD-6000-Shimadzu model, Co K_α radiation (λ = 1.78897 Å), 30 kV and 30 mA on Bragg-Brentano geometry. The variations of the peaks intensity were measured with $\theta/2\theta$ coupled, between 40º and 110º of 2θ with 0.02º step on continuous scanning. Based on literature,[15] the phases associated to the planes were identified as:

- Austenite (faced-centered cubic – FCC - γ - A): (111), (200) e (220);
- Martensite (body-centered cubic – BCC - α' - M): (110), (200) e (211).

The intensity, area and width of half height, for austenite and martensite XRD peaks, were verified with "Spectroscopy / Baseline and Peaks" functions on the OriginPro 8 Software.

3 RESULTS AND DISCUSSION

The Figure 2 shows the uniaxial tensile curves for the austenitic stainless steel as a function of the strain-rate. Table 3 summarizes the mechanical properties obtained from the figure 1 and tensile specimens gauge length measurements after tests.
The tensile test at different strain rate at room temperature gives rise to different behaviors in true stress-strain curves (Figure 2). The test performed at 5.55 x 10^{-4} s^{-1} strain rate (IN-L tensile specimen) shows smaller yield strength and higher true tensile stress and total true strain when compared with 5.55 x 10^{-3} s^{-1} strain-rate. Near to 1,000 MPa, the IN-L1 tensile specimen (5.55 x 10^{-3} s^{-1} strain-rate) presented a softening.

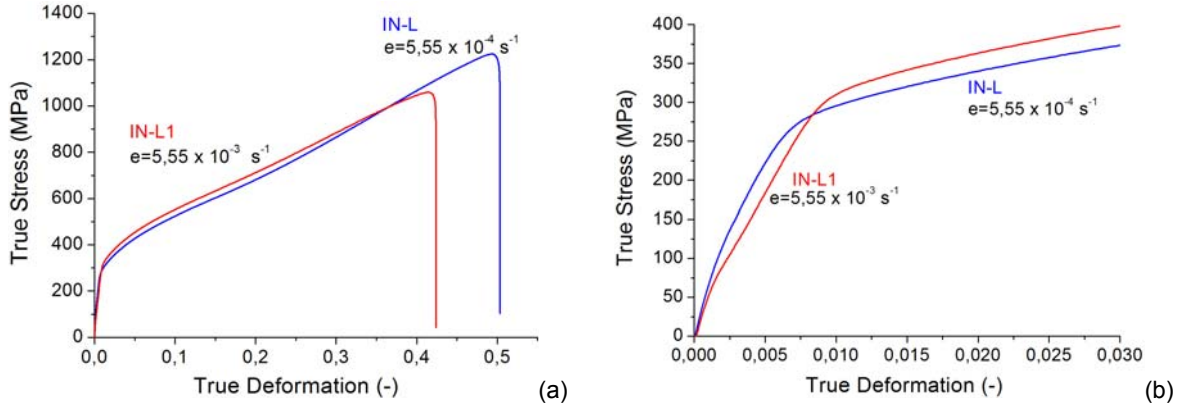

Figure 2. Uniaxial true stress-true strain results as a function of two strain-rates: (a) up to failure and (b) the elastic zone and at the beginning of plastic zone deformation.

The Figure 2b reveals that the tensile test with different strain rate distinct behavior on elastic zone beyond plastic zone (Figure 2a). The IN-L tensile specimen deformed with 5.55 x 10^{-4} s^{-1} strain-rate has higher elastic stiffness that IN-L1 tensile specimen

ISSN 1516-392X

deformed with 5.55 x 10^{-3} s^{-1} strain-rate. This behavior can be attributed to strain-rate influence and/or small difference on initial martensite fraction in each sample.

Table 3. AISI 304L uniaxial tensile mechanical properties

Sample, Strain Rate	Yield stress (MPa)	Ultimate tensile stress (MPa)	Total elongation(%)
IN-L, 5.55 x 10^{-4} s^{-1}	284	1225	50.3
IN-L1, 5.55 x 10^{-3} s^{-1}	324	1058	42.4

Based on ferritoscope in-situ measurements during tensile test in the 10%, 25%, 50%, 75% and 90% intervals between yield and maximum loads (Table 2 – Material and Methods Section), Table 4 summarizes the initial and final martensite fraction values. All tensile specimens had distinct initial martensite fraction (minimum: 0.42; and maximum: 0.61%). The tensile specimens deformed with 5.55 x 10^{-4} s^{-1} strain-rate have higher values of final martensite fraction at same percent load stop condition.

Table 4. Initial and Final Martensite (α') Fraction measured, during tensile tests at distinct load stop (between yielding and maximum load before narrowing) and strain rate, with ferritoscope in-situ measurements

Tensile Test Sample - Stop Condition*	Martensite Fraction (%)		Strain Rate (s^{-1})
	Initial	Final	
IN-L4 - (10% / 462.1 MPa / 123.2 s)	0.58	0.90	5.55x10^{-4}
IN-L6 - (25% / 588.0 MPa / 264.3 s)	0.45	1.76	
IN-L3 - (50% / 708.5 MPa / 427.7 s)	0.48	6.85	
IN-L5 - (75% / 871.5 MPa / 631.3 s)	0.53	14.72	
IN-L2 - (90% / 1052.8 MPa / 861.0 s)	0.61	23.57	
IN-L9 - (10% / 501.9 MPa / 13.6 s)	0.46	0.84	5.55x10^{-3}
IN-L11 - (25% / 588.3 MPa / 23.4 s)	0.52	1.60	
IN-L8 - (50% / 675.5 MPa / 35.0 s)	0.42	3.22	
IN-L10 - (75% / 793.2 MPa / 50.8 s)	0.56	7.72	
IN-L7 - (90% / 936.9 MPa / 70.0 s)	0.50	11.94	

** % (Maximum Load – Yielding Load) / True Stress / Time.*

The Figures 3 and 4 show the true stress *versus* time curves associated with martensite formation evolution measured with ferritoscope during tensile test at 5,55 x 10^{-4} and 5,55 x 10^{-3} s^{-1} strain-rate up to 10% and 90% load stop condition, respectively. The tensile specimens deformed with 5,55 x 10^{-3} s^{-1} strain-rate (Figures 3b and 4b) induced smaller quantity of martensitic transformation, during all steps of tensile test, than 5,55 x 10^{-4} s^{-1} strain rate (Figures 3a and 4a).

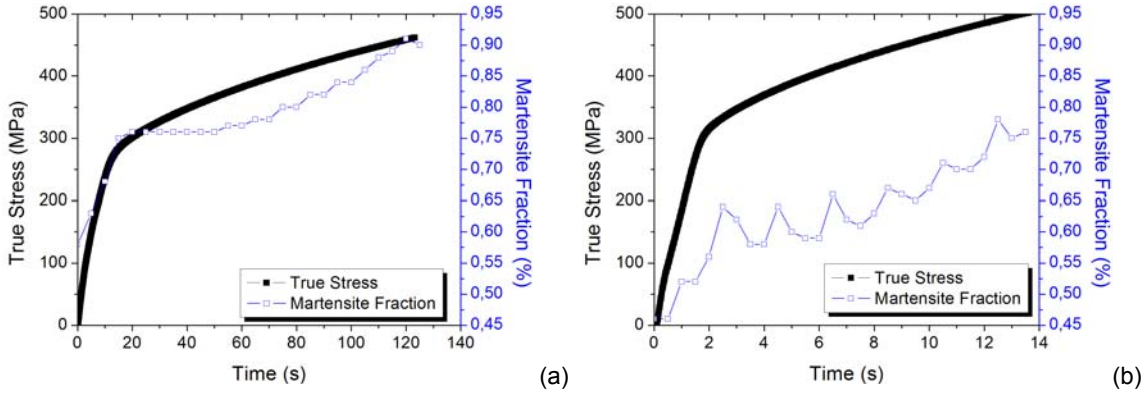

Figure 3. Mechanical Behavior in tensile test associated with martensite fraction formed during tensile test up to 10% load between maximum and yielding load and rate deformation of (a) 5,55 x 10^{-4} s^{-1} (IN-L4) and (b) 5,55 x 10^{-3} s^{-1} (IN-L9).

ISSN 1516-392X

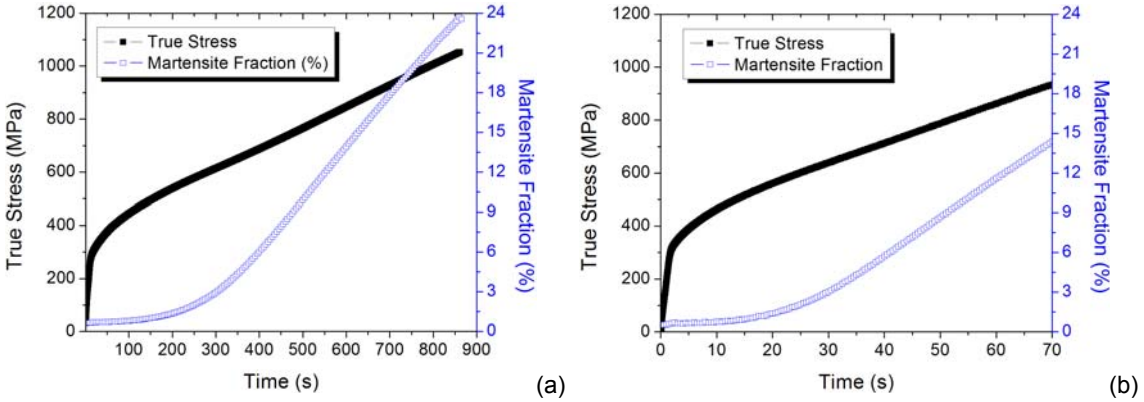

Figure 4. Mechanical Behavior in tensile test associated with martensite fraction formed during tensile test up to 90% load between maximum and yielding load and rate deformation of (a) 5,55 x 10^{-4} s^{-1} (IN-L2) and (b) 5,55 x 10^{-3} s^{-1} (IN-L7).

The figure 5a,c-f shows the microstructural aspects of austenitic stainless steel in study in as-received condition and after tensile tests with distinct and load stop condition selected (10% and 90%) at distinct strain rates (5,55 x 10^{-4} and 5,55 x 10^{-3} s^{-1}). As-received sample (Figure 5a) presents austenitic matrix with some twins and small evidences of martensite by needle regions inside austenitic grains. The microstructural aspects after tensile tests (Figures 5c to 5f) reveal an increased of the needle regions and flattening on austenite grain surface associated with increased of the load stop condition and decreased of the strain rate (5,55 x 10^{-4} s^{-1}), but if the strain rate increase implies on more austenitic grain surface flatten related to an increase on mechanical hardening by dislocation motion and interaction.
Figure 5b shows the Vickers microhardness evolution from as-received and tensile tests with distinct strain rate and load stop condition. These results reveal the increased of hardness with load stop condition associated with increment on the deviation pattern for intermediate load stop condition (25% and 50%). However, as-received sample has a smaller deviation pattern; this behavior can be attributed to present phase and mechanical hardening level on non-transformed austenite. The hardness values are highest for high strain rate (5,55 x 10^{-3} s^{-1}) up to 25% load stop condition. The hardness results are in concordance with mechanical behavior on tensile tests (Figure 2a).

ISSN 1516-392X

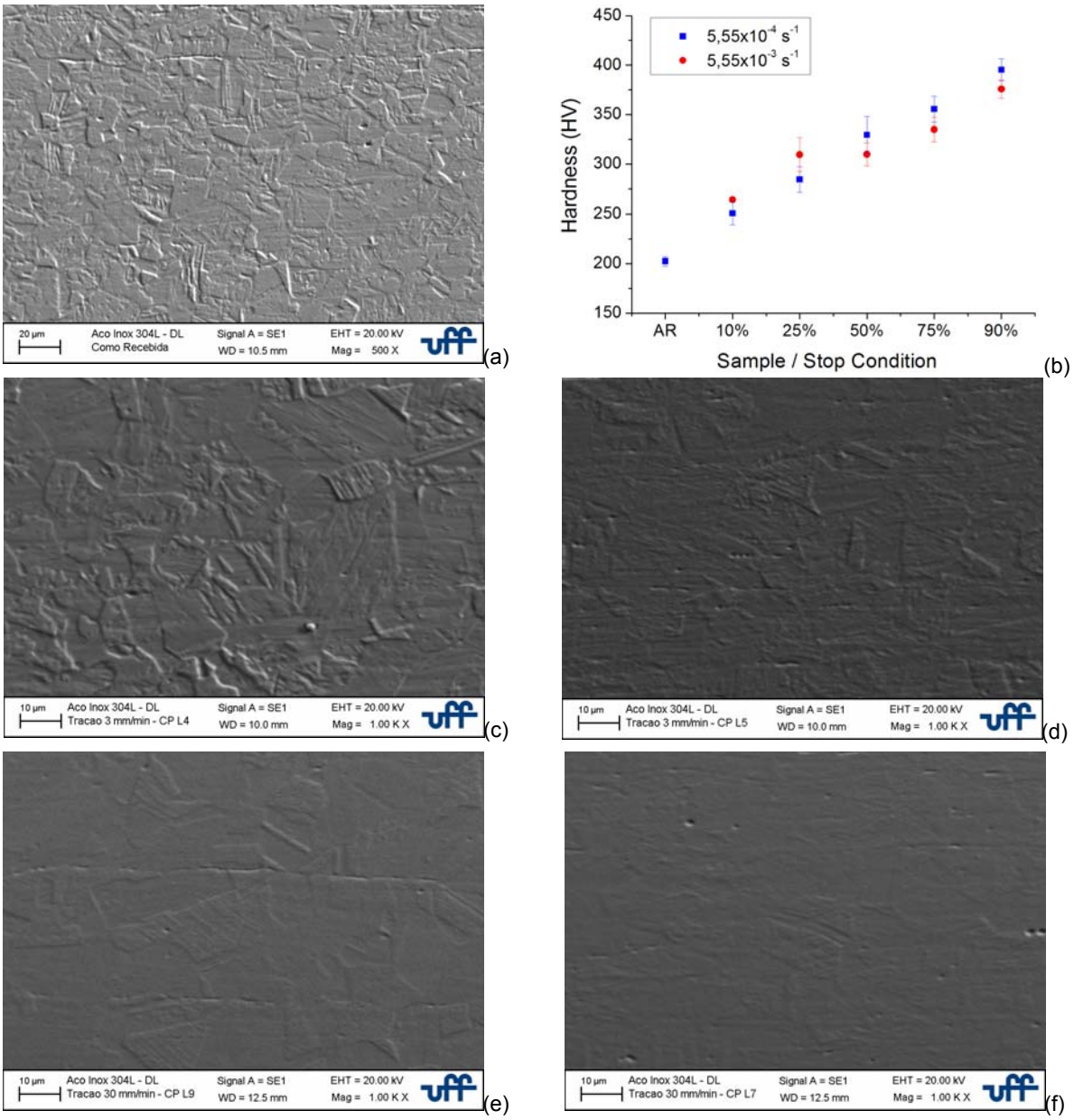

Figure 5. Microstructural aspects associated to mechanical evolution of steel in study on the following conditions: (a) as-received; and after tensile tests in distinct load stop conditions between YL and ML: (c-d) 10% and 90% with 5,55 x 10^{-4} s^{-1} rate strain, and (e-f) 10% and 90% with 5,55 x 10^{-3} s^{-1} rate strain. (b) Hardness evolution as a function of load stop condition increment on tensile tests at 5,55 x 10^{-4} and 5,55 x 10^{-3} s^{-1} rate strain.

The Figures 6 and 7 show the DRX results for the as-received (AR) and loaded conditions. AR sample has austenitic peaks (A - (111), (200) and (220)) predominance when compared with intensity martensitic peaks (M - (110) and (211)). After tensile tests with increasing of load stop condition, XRD analysis verified that austenitic peaks (A – (111), (200) and (220)) decrease, (200) martensitic peak appear above 25% load stop condition and martensitic peaks (M – (110), (200) and (211)) increase.

ISSN 1516-392X

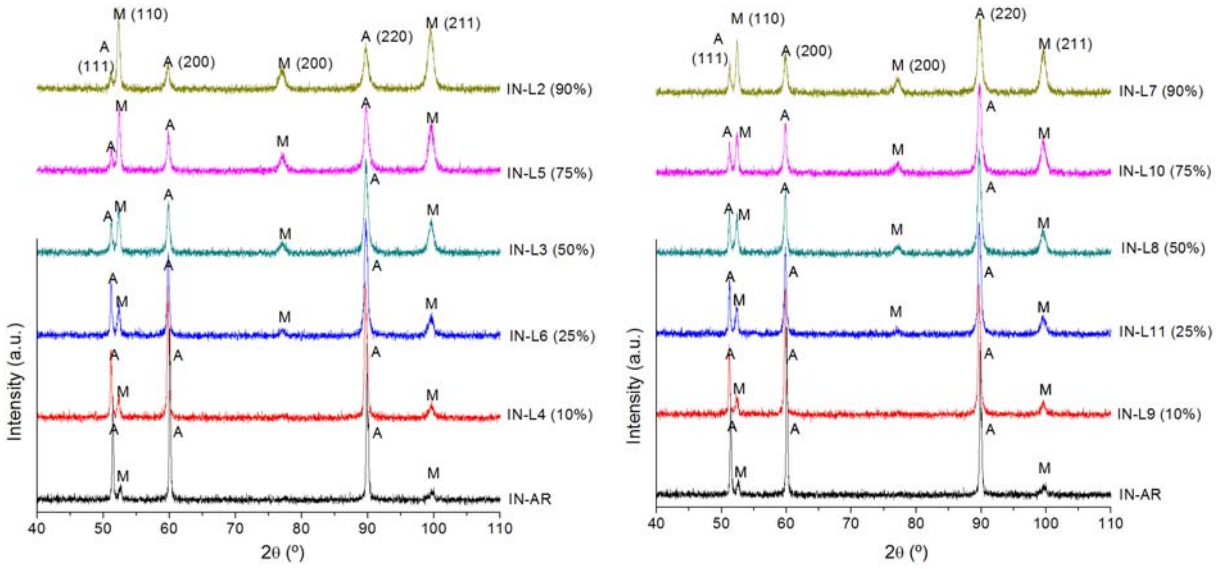

Figure 6. X-Ray Diffraction Spectrum of the tensile test sample submitted at distinct load stop conditions (between yielding and maximum load before narrowing) and rate strain: (a) 5,55 x 10^{-4} and (b) 5,55 x 10^{-3} s^{-1} rate strain. A = Austenite (γ). M = Martensite (α').

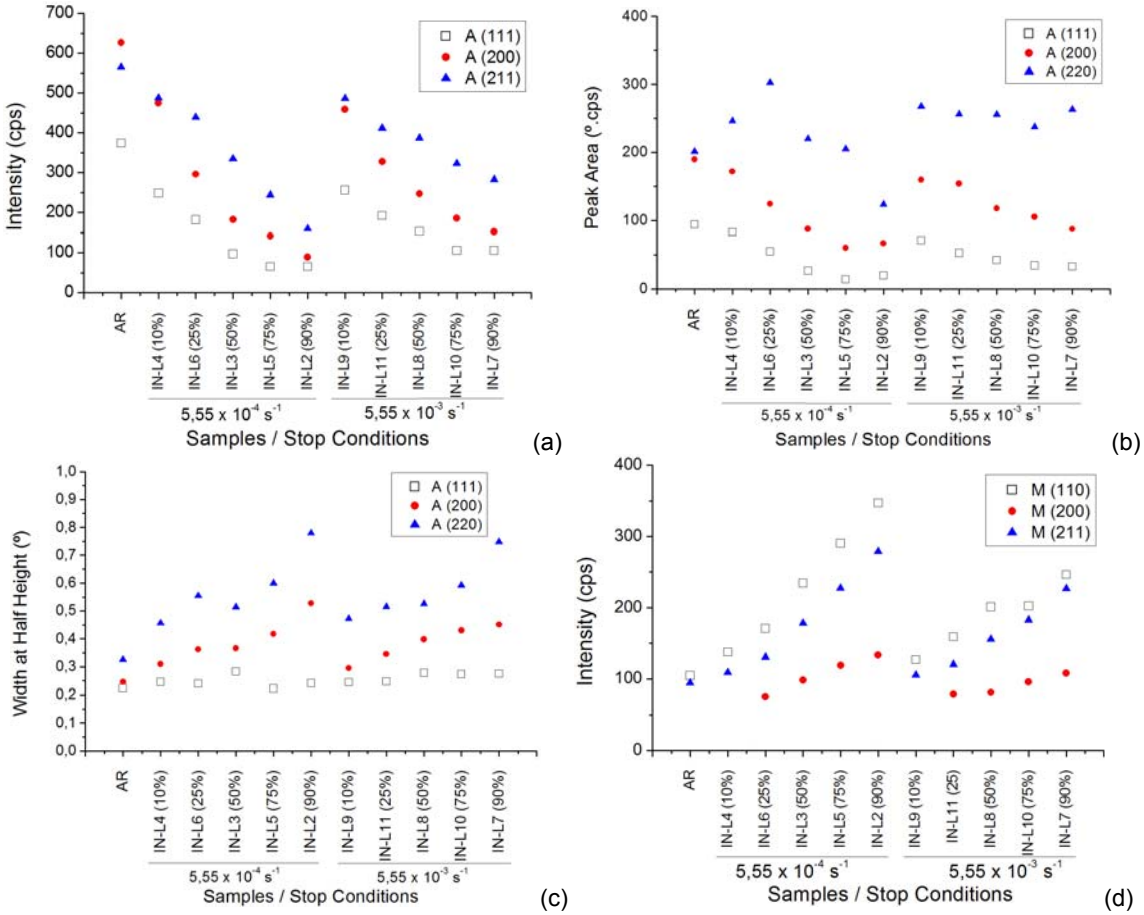

Figure 7. Evolution of Austenite consumed as a function of peak (a) intensity, (b) area, and) (c) width at half height, of the diffracted planes with (111), (200) and (220) orientations parallel to sheet surface. (d) Evolution of Martensite formation as a function of peak intensity of diffracted planes with (110), (200) and (211) orientations parallel to sheet surface. A = Austenite (γ). M = Martensite (α').

Figures 7a to 7c show the graphics with the evidence of austenite consumed evolution after tensile test with distinct strain rate and load stop conditions compared

ISSN 1516-392X

with AR sample, associated to intensity, area and width at half height of austenitic peaks with (111), (110) and (220) orientations. Its possible noticed that a decreased on intensity and area peak diffracted as a function of the load stop condition increased and strain rate decreased (5.55 x 10^{-4} s^{-1} strain rate). The width at half height is related with the crystal distortion associated to mechanical hardening level. Thus is possible to infer that the austenite grain associated with (110) and (220) orientation exhibit high distortion with load stop condition increased and strain rate decreased (5.55 x 10^{-4} s^{-1} strain rate), while the (111) orientation keep constant.
In Figure 7d is shown the martensite formation evolution by diffract peak increment associated with (110), (200) and (211) martensite peak orientation. It's possible to verify a progressive increased on the peak intensity with load stop condition increased and strain rate decreased (5.55 x 10^{-4} s^{-1} strain rate). This behavior is in agreement with ferritoscope measurements.
According to the literature,[16,17] the Bain deformation, on FCC to BCC martensitic transformation, results in the correspondence of crystal plane: $(111)\gamma \rightarrow (011)\alpha'$. Its is clearly to verify in the XRD results that (111) austenite peak is the orientation more consumed than others (Figures 7a and 7c) and (110) martensite peak is the orientation more preeminent formation that others (Figure 7d). However, its necessary another specify techniques to infer in the orientation relation between austenite and martensite during this experimental work.
The tensile test results (Figure 2a), are in agreement with the literature,[12-15,18,19] this behavior can be attribute to a higher exothermic heat generated by the slips and dislocation interactions as a function of strain rate increases during mechanical deformation, that promote a much higher increase in tensile specimen temperature. When the tensile specimen temperature to approach the M_d temperature, the austenite free energy increase and the strain to induce the martensitic transformation increase too, in this way it is necessary a higher local mechanical hardening before start martensitic transformation. This behavior is clearly shown by XRD results associated to non-transformed austenite peak profile (Figure 7a-c), where (111), (110) and (220) austenite peak orientations shows higher intensity with increase of deformation and strain rate.

4 CONCLUSIONS

Based on the uniaxial tensile tests conducted on a 304L austenitic stainless steel sheet with two strain rates (5.55 x 10^{-3} and 5.55 x 10^{-4} s^{-1}), the following conclusions can be drawn:

- the as-received condition exhibited a small fraction of martensite (< 1%), which promoted small changes in the elastic and yielding behavior during tensile tests;
- strain rate increased in tensile tests promote an initial increasing on the yield strength, however in the final deformation stages occurred a change – the low strain rate assumed high mechanical resistance to deformation;
- lower strain rate in study made possible an higher martensite volume fraction formed during the deformation process;
- higher strain-rate associated to the higher austenite hardening and an apparent increased on the tensile specimen temperature were probable the responsible to smaller martensite volume fraction, mainly in the last stage of the plastic deformation;

ISSN 1516-392X

- the austenite grains with (111) planes parallel to sheet surface shown potential evidences of a high conversion level on martensite and low mechanical hardening level on its non-transformed condition.

Acknowledgments

The authors wish to acknowledge the financial support from CNPq (Universal Grant 471889/2010-5, Scientific Initiation scholarship (G.A.M.), and PQ2 Research Grant (L.P.M.)), Capes (Master scholarship (M.C.C.)) and Faperj (Technological Initiation scholarship (J.G.A.), E-26/160.020/2010) Brazilian agencies, Arcelor Mittal Inox Brasil S.A. for material supply, Companhia Siderúrgica Nacional for tensile test samples preparation and UniFOA for tensile tests execution.

REFERENCES

1 COHEN, M.; WAYMAN, C.M.; Fundamentals of Martensitic Reactions, Published in: Treatises in Metallurgy, J.K. Tien and J.F. Elliot, 1981.
2 HONEYCOMBE, R.W.; BHADESHIA, H.K.DH; Steels, Microstructure and Properties. London: Edward Arnold, 1981.
3 CINA, B.; J. Iron Steel Inst. (1954) 791.
4 CHERKAOUI, M.; BERVEILLER, M.; SABAR, H.; Micromechanical Modelling of Martensitic Transformation Induced Plasticity (TRIP) in Austenitic Single Crystals, International Journal of Plasticity, Vol. 14, Nº 17, pp. 597-626, 1998.
5 MANGONON, P.J.; THOMAS, G.; The Martensite Phases in 304 Stainless Steel, Metallurgical Transactions, 1 (1970) pp. 1577-1586.
6 ANGEL, T.; Formation of Martensite in Austenitic Steels, J. Iron Steel Inst., 5 (1954) pp. 165-174.
7 KRUPP, U.; WEST, C.; DUAN, H.P.; CHRIST, H.J.; Strain-induced Martensite Formation in Metastable Austenitic Steels with varying Carbon content, Z. Metallkd, 7 (2002) pp. 706-711.
8 KRUPP, U.; CHRIST, H.P.; LEZUO, P.; MAIER, H.J.; TETERUK, R.G.; Influence of Carbon Concentration on Martensitic Transformation in Metastable Austenitic Steels under Cyclic Loading Conditions, Materials Science and Engineering A, 319-321 (2001) pp. 527-530.
9 FISCHER, F.D.; SUN, Q.P.; TANAKA, K.; Transformation-Induced Plasticity (TRIP), ASME Applied Mechanical Review, 49, 317.
10 FISCHER, F.D.; REISNER, G.; WESNER, E.; TANAKA, K.; CAILLETAUD, G.; ANTRETTER, T.; A New View on Transformation Induced Plasticity (TRIP), International Journal of Plasticity, 16 (2000), pp. 723-748.
11 OLSEN, G.B.; COHEN, M.; Kinetics of Strain-induced Martensitic Nucleation, Metallurgical Transaction A, 6A (1975) pp. 791-795.
12 LICHTENFELD, J.A.; MATAYA, M.C.; VAN TYNE, C.J.; Effect of Strain Rate on Stress-strain Behavior of Alloy 309 and 304L Austenitic Stainless Steel, Metallurgical Transaction A, 37A (2006), pp. 147-161.
13 McREYNOLDS, A.W., Effect of Stress and Deformation on the Martensitic Transformation, J. Appl. Phys., 20 (1949) pp. 896-907.
14 ANDRADE-CAMPOS, A.; TEIXEIRA-DIAS, F.; KRUPP, U.; BARLAT, F.; RAUCH, E.F.; GRÁCIO, J.J.; Effect of Strain Rate, Adiabatic Heating and Phase Transformation Phenomena on the Mechanical Behaviour of Stainless Steel, Strain, 46 (2010) pp. 283-297.
15 RYOO, D.; KANG, N.; KANG, C.; Effect of Ni content on Tensile Properties and Strain-induced Martensite Transformation for 304 Stainless Steel, Materials Science and Engineering A, 528 (2001) p. 2277.

ISSN 1516-392X

16 PORTER, D.A.; EARSTELING, K.E.; Phase Transformations in Metals and Alloys, Chapman & Hall, 2nd Edition, 1992.
17 BAIN, E.C; Trans AIME, 70 (1924) p. 25.
18 IWAMOTO, T.; TSUTA, T.; TOMITA, Y.; Investigation of deformation mode dependence of strain-induced martensitic transformation in trip steels and modelling of transformation kinetics, International Journal of Mechanical Sciences 40/2-3 (1998) p. 173.
19 MOREIRA, L.P.; MERCIER, S.; MEDEIROS, N.; MARTINY, M.; MATTOS, E.B.; "Análise Numérica da Estampagem de Chapas de Aços com Efeitos de Transformação de Fases", In: VI Congresso Nacional de Engenharia Mecânica, 2010 – Paraíba / Brazil.